ANNUAL REVIEWS Further
Click here for quick links to Annual Reviews content online, including:
• Other articles in this volume
• Top cited articles
• Top downloaded articles
• Our comprehensive search

The Uses of Dynamic Earthquake Triggering

Emily E. Brodsky[1] and Nicholas J. van der Elst[2]

[1]Department of Earth & Planetary Sciences, University of California, Santa Cruz, California 95064; email: brodsky@es.ucsc.edu

[2]Lamont-Doherty Earth Observatory, Columbia University, Palisades, New York 10964; email: nicholas@ldeo.columbia.edu

Annu. Rev. Earth Planet. Sci. 2014.42:317-339. Downloaded from www.annualreviews.org
Access provided by Pennsylvania State University on 10/26/15. For personal use only.

Annu. Rev. Earth Planet. Sci. 2014. 42:317–39

First published online as a Review in Advance on February 24, 2014

The *Annual Review of Earth and Planetary Sciences* is online at earth.annualreviews.org

This article's doi:
10.1146/annurev-earth-060313-054648

Copyright © 2014 by Annual Reviews.
All rights reserved

Keywords

earthquakes, stress in the crust, friction

Abstract

Dynamic triggering of earthquakes by seismic waves is a robustly observed phenomenon with well-documented examples from over 30 major earthquakes. We are now in a position to use dynamic triggering as a natural experiment to probe the reaction of faults to the known stresses from seismic waves. We show here that dynamic triggering can be used to investigate the distribution of stresses required for failure on faults. In some regions, faults appear to be uniformly distributed over their loading cycles with equal numbers at all possible stresses from failure. Regions under tectonic extension, at the interface between locked and creeping faults, or subject to anthropogenic forcing are most prone to triggered failure. Predictions of future seismicity rates based on seismic wave amplitudes are theoretically possible and may provide similar results to purely stochastic prediction schemes. The underlying mechanisms of dynamic triggering are still unknown. The prolonged triggered sequences require a multistage process such as shear failure from rate-state friction coupled to aseismic creep or continued triggering through a secondary cascade. Permeability enhancement leading to drainage or pore pressure redistribution on faults is an alternative possibility.

Annu. Rev. Earth Planet. Sci. 2014.42:317-339. Downloaded from www.annualreviews.org
Access provided by Pennsylvania State University on 10/26/15. For personal use only.

INTRODUCTION TO OBSERVATIONS OF DYNAMIC TRIGGERING

What controls the timing of earthquakes? Earthquakes occur when the elastic stress in plates driven by long-term motion overcomes the failure stress of faults. This general picture has been well established since the discovery of plate tectonics. In this framework, earthquake behavior appears predictable. If the strength, stress drop, and rate of stress accumulation are all constant, then earthquakes should occur with a well-defined periodicity (**Figure 1**). However, this simple picture does not seem to apply to natural settings. Merely measuring the rate of motion of faults and calculating the strength and stress drop from rock properties has proved an unsatisfactory method of earthquake prediction.

This lack of success may stem from the variations in loading, rock strength, and dynamic friction over time and space. For instance, the loading rate may be variable due to interactions with neighboring faults. The strength depends on local lithology and may evolve due to healing and redamaging processes in fault zones. The stress drop that determines the starting point for each cycle is dependent on both the lithology and the dynamic properties of friction. So, how are we to proceed?

One strategy is to attempt to measure the stress on faults in situ by using the response to known perturbations of the stress field. Raleigh et al. (1976) pioneered this approach for the special case of anthropogenic seismicity and found that the rock mechanics failure thresholds were applicable given appropriate assumptions. However, the distribution of unperturbed stresses cannot be accessed by this method, nor can human perturbations be utilized on a broad scale.

Another approach is to use dynamic triggering of earthquakes as a probe of the stresses on faults. It has been well demonstrated that seismic waves can trigger earthquakes since the 1992 M_w 7.3 Landers earthquake in southern California over 20 years ago. Within minutes after the mainshock, earthquakes occurred throughout the western United States in locales as far away as Yellowstone Caldera (>1,500 km distant), and the regional earthquake rate was elevated for days

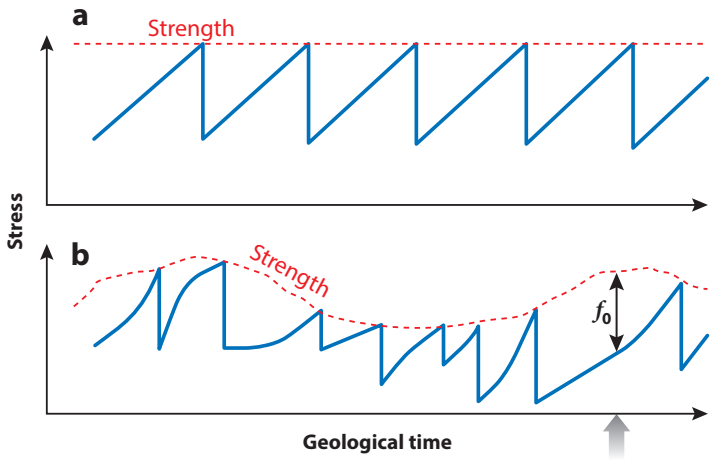

Figure 1

Schematic of the state of stress and strength on a fault. (*a*) A fault with a constant loading rate, stress drop, and strength. Perfectly periodic failure results. (*b*) A fault with variable loading rate, stress drop, and strength. More complex earthquake behavior results. If a distant earthquake provides a triggering stress s that exceeds f_0 at the time of the gray arrow, immediate slip will occur. In general, the minimum stress f required to drive a fault to failure may depend on the history (state) of the fault and therefore can be greater or less than f_0. Adapted with permission from Kanamori & Brodsky (2001). Copyright 2001, American Institute of Physics.

Annu. Rev. Earth Planet. Sci. 2014.42:317-339. Downloaded from www.annualreviews.org
Access provided by Pennsylvania State University on 10/26/15. For personal use only.

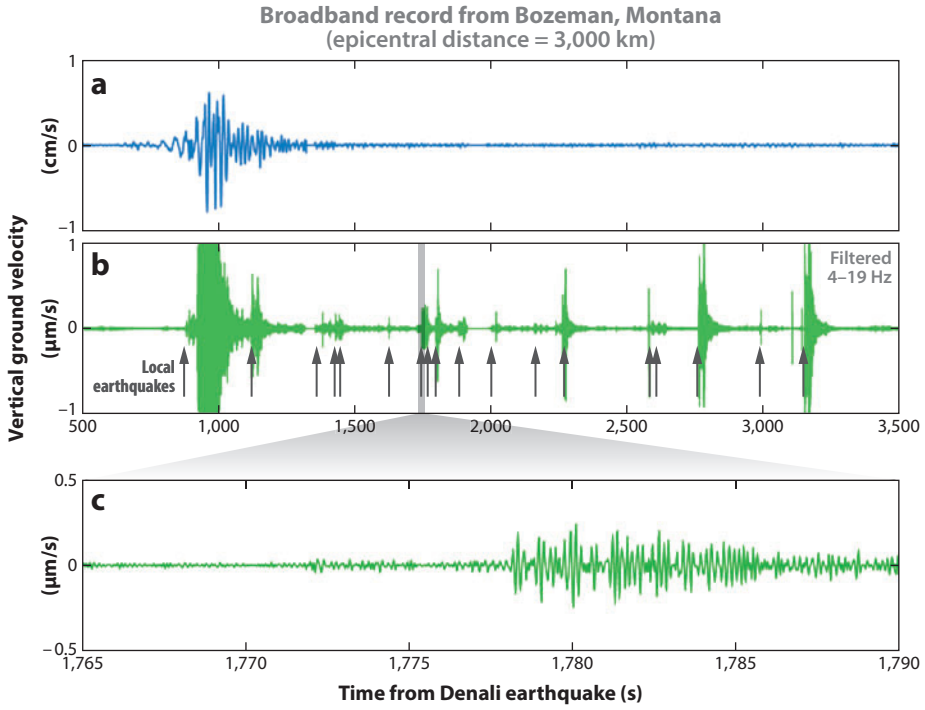

Figure 2

Example of dynamic triggering from the 2002 M_w 7.9 Denali earthquake. (*a*) The original record is dominated by the long-period waves from the mainshock. (*b*) The high-passed version shows the local earthquakes (*gray arrows*). (*c*) The close-up shows that the events marked by gray arrows have well-defined *P* and *S* arrivals that allow the events to be located and analyzed. Modified from Manga & Brodsky (2006).

(Hill et al. 1993). These earthquakes were much further away than the conventional aftershock zone, which extends only a few fault lengths away from the mainshock (up to a couple hundred kilometers in the case of the Landers quake). The great distances involved and the rapidity of the triggering led researchers to quickly determine that the seismic waves were the source of the triggering stress.

The Landers earthquake was remarkable because it was the first major event in the era of modern, dense networks. The improved density of seismic instrumentation allowed seismologists to detect the predominantly small earthquakes hiding in the aftermath of a large earthquake. Since Landers, dynamic triggering has been documented following over 30 major earthquakes (Gomberg et al. 2001, 2004; Freed 2005; Pollitz et al. 2012; Prejean & Hill 2009; van der Elst et al. 2013a; Velasco et al. 2008; West et al. 2005; Wu et al. 2011). Often the triggered events ride on the surface wave train. For instance, in **Figure 2** the waves from the 2002 M_w 7.9 Denali earthquake were recorded on a seismometer in Montana near the Yellowstone Caldera. The top panel shows the broadband record, which is dominated by the long-period waves traveling from the mainshock. The middle panel shows the same data through a high-pass filter that removes the long-period waves. The high-frequency energy that remains must be originating close to the seismometer, because the high-frequency waves from the distant mainshock attenuate rapidly in the crust. Magnification of individual triggered events shows well-defined *P* and *S* arrivals that allow location and magnitude determination of the earthquakes. The timing of the local events

provides further evidence that the seismic waves are triggering the local events. Occasionally pulses of earthquakes are seen synchronized with individual surface wave packets (West et al. 2005).

In **Figure 2**, the triggered events continue even after the seismic waves have passed. There are also examples of unusual increases of earthquake rate apparently beginning hours or days after large ground motions (Prejean & Hill 2009, Pollitz et al. 2012). Dynamic triggering encompasses all statistically significant increases in earthquake rate for which a statistical or physical constraint implies that the seismic waves are the trigger.

Now that dynamic triggering is a well-documented phenomenon, we are in a position to begin to use it as a probe of the natural system. Seismic waves are readily observable by seismometers, and the elastic stresses in the waves can be estimated from ground motion combined with the elastic properties of rocks. For instance, for an SH wave propagating in the x direction with displacement $u = u_0 \exp[i(\omega t - kx)]$, where ω is the angular frequency and k is the wavenumber, the peak shear strain is proportional to the magnitude of the spatial derivative of the displacement field, i.e., proportional to ku. Because the wavenumber $k = \omega/c$, where c is the phase velocity, the strain is proportional to the magnitude of the particle velocity (ωu) of the wave. The elastic shear stress is therefore also proportional to the particle velocity. For more complex waves in 3D, a similar argument holds and the terms of the stress tensor are proportional to the components of particle velocity. We can measure how many earthquakes are triggered by these ground motions and therefore how many faults had initial stress states that required only the observed stress of the seismic wave to drive them to failure.

The mechanisms by which dynamic triggering occur are currently unknown. Possibilities include direct stressing to failure, damage and weakening of the fault zone, or a more complex cascade of stressing and fluid processes. We return to this topic at the end of this article. For the purpose of probing faults, the important observation is that a given stress results in a given earthquake rate. Recognizing that the stress may operate on the fault through a highly nonlinear sequence of steps, we refer to the stress f required to make a given fault fail as the stress from failure. In the simplest case of direct Coulomb shear failure in response to the seismic wave, f is the difference between the pretrigger stress and strength shown by f_0 in **Figure 1**. More generally, f may reflect the minimum transient stress required to initiate fault creep or weakening that ultimately leads to a triggered earthquake. Even in this complex case, the path to failure depends on the initial stress state, and therefore information about the in situ stress and strength can be derived from observations of f.

To measure f with dynamic triggering, we must first establish whether the number of triggered faults behaves systematically as a function of the stress of the incoming waves. Do larger amplitude waves trigger more earthquakes? This question was explored by van der Elst & Brodsky (2010). In that work we developed a metric of rate changes based on the interevent times of populations. We identified times of known ground shaking in California due to distant earthquakes and at each time measured the statistic R,

$$R = t_2/(t_1 + t_2), \tag{1}$$

at locations in California, where t_2 is the time between a distant mainshock and the next local earthquake in the Californian region and t_1 is the time between the previous local, Californian earthquake and the distant mainshock (Felzer & Brodsky 2005, Frohlich & Davis 1985). For any specific instance of shaking, R is a random variable. If there is no effect of the distant earthquake on the local seismicity, R is uniformly distributed between 0 and 1. If triggering is present, R is biased toward a smaller value. A larger triggering rate generates a larger bias.

The bias can be measured by the mean value of R for a group of potential triggering times or areas. Triggering earthquakes that generate the same ground motion can be grouped and the

Annu. Rev. Earth Planet. Sci. 2014.42:317-339. Downloaded from www.annualreviews.org
Access provided by Pennsylvania State University on 10/26/15. For personal use only.

average value of R measured for the group. This average value of R can be related to a fractional rate change given a statistical model for event recurrence. If the triggering process is a step change in the rate of a Poissonian process, the expected value of R is

$$\langle R \rangle = \frac{1}{n^2}[(n+1)\ln(n+1) - n], \tag{2}$$

where

$$n \equiv \frac{\lambda_2 - \lambda_1}{\lambda_1}, \tag{3}$$

λ_1 is the earthquake rate prior to the perturbation, and λ_2 is the earthquake rate afterward (van der Elst & Brodsky 2010). The fractional rate change n is uniquely determined by a measurement of the average value of R in a group of potentially triggered earthquakes that experienced the same perturbing stress.

The data for California show a systematic increase in triggered earthquake rate as a function of amplitude of the triggering stress (**Figure 3**). The fact that this trend is continuous and smooth despite the variety of spectra and orientations of the stress fields is important. More specialized studies have investigated triggering differences based on wave frequency and duration (Aiken et al. 2013, Brodsky & Prejean 2005, Gomberg & Davis 1996, Gomberg & Felzer 2008, Prejean & Hill 2009). **Figure 3** shows that the more complex attributes of the waveform do not overwhelm the average behavior of a sufficiently large data set. The amplitude by itself is a good predictor of average behavior and can be used to measure f in the crust.

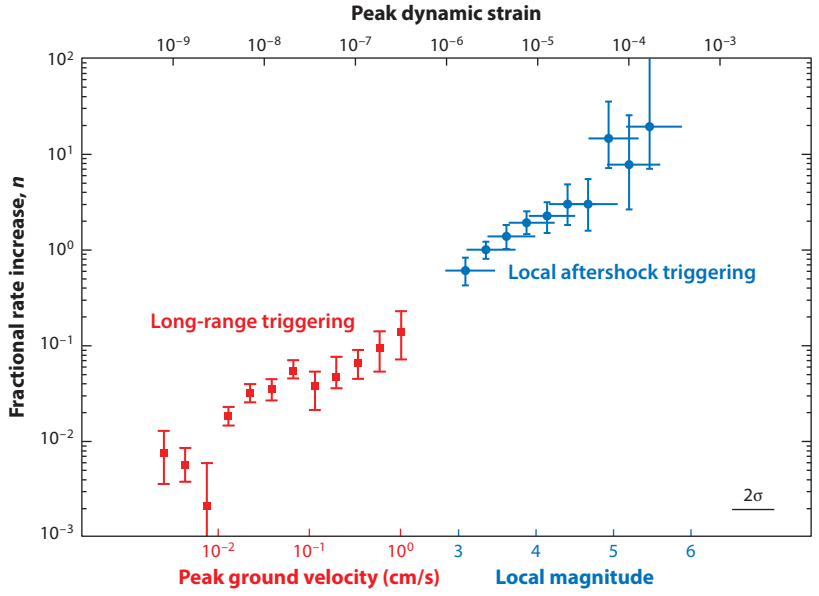

Figure 3

Triggered earthquake rate change (n of Equation 3) in California measured using the R statistic (Equation 2). Data are from the Advanced National Seismic System (ANSS) earthquake catalog between 1984 and 2009, using a magnitude cutoff of 2.1. Long-range triggering (*red*) is at least 800 km distant; local (*blue*) is less than 6 km. Peak dynamic strain is measured from appropriate empirical ground motion regressions. Modified from Manga et al. (2012) as adapted from van der Elst & Brodsky (2010). Note that van der Elst & Brodsky (2010) used an approximately constant number of samples per bin, but this recalculation of the figure uses bins with a consistent range of strain in log space.

Annu. Rev. Earth Planet. Sci. 2014.42:317-339. Downloaded from www.annualreviews.org
Access provided by Pennsylvania State University on 10/26/15. For personal use only.

Now that we have established that dynamic triggering behaves systematically, we can begin to use it to examine the in situ state of stress on faults. In this article we explore four different applications along this line: (1) measuring the distribution of fault stress from failure f, (2) identifying regional differences in f in order to elucidate the role of tectonics and other processes in controlling f, (3) predicting earthquakes, and (4) constraining the physics of earthquake nucleation.

APPLICATION 1: THE DISTRIBUTION OF f IN THE CRUST

The distribution of fault stresses in the crust is a long-standing problem. There is a physical expectation that a regular loading cycle should dominate long-term behavior, but some argue that the crust is near failure everywhere (Reid 1911, Townend & Zoback 2000). As a large variety of faults are present in any section of crust, it is possible that cyclic loading leads to a distribution of stress from failure, with some number of faults always near critical. Dynamic triggering provides insight into the distribution.

We see that the observable fractional rate change in California, as measured by Equation 2, is proportional to the square root of the perturbing stress, which we call s. However, this scaling was based on the naive application of a Poissonian step-change approximation to a highly nonhomogeneous earthquake population (van der Elst & Brodsky 2010). Statistical simulations show that the square-root scaling of the time ratio measurement based on R is consistent with a linear scaling between s and the number of activated faults. The exact scaling is model dependent, and therefore to confirm the scaling between the number of events and perturbing stress s, we turn to other measurements.

The total number of aftershocks following a mainshock is consistent with triggering rate scaling linearly with s (**Figure 4**). Aftershock productivity is linear with 10^M, where M is magnitude (Felzer et al. 2004, Helmstetter et al. 2005, Reasenberg & Jones 1990). As regional magnitude was originally defined on the basis of the common logarithm of the peak seismic wave amplitude at a fixed frequency, aftershock productivity is proportional to the dynamic stress. Similarly, aftershock decay away from the fault can be predicted by the peak stress, or by a combination of peak stress and duration (Felzer & Brodsky 2006, Gomberg & Felzer 2008). The number of excess events triggered by tidal stresses also increases approximately linearly with the peak Coulomb stress acting on the faults (Cochran et al. 2004, Stroup et al. 2007).

A perturbing stress of a specific amplitude will sweep to failure all faults with f less than or equal to that value. Therefore, the observation constrains the integral

$$n = \frac{1}{N_T} \int_0^s N(f) df, \tag{4}$$

where n is the fractional rate change defined by Equation 3, $N(f)$ is the number of faults with a given value of f, and N_T is the total number of faults. The observations indicate that the integral in Equation 4 is linear in s and therefore $N(f)$ is constant.

In statistical terms, $N(f)$ being constant implies that the distribution of faults is uniform over all observed values of f and an arbitrary fault selected at random has an equal probability of being at any value of f. This situation can occur if faults are uniformly loaded over time and have a consistent failure threshold (**Figure 1*a***) and if there are a sufficient number of faults in the system that they are evenly distributed over their loading cycles. A similar model was assumed by Dieterich (1994); now, dynamic triggering provides observational evidence supporting the assumption.

This statistical interpretation of the triggering rates implies that the number of triggered earthquakes in an area should be proportional to the background earthquake rate in that area. In this interpretation, a higher background rate indicates more faults near failure and therefore

Annu. Rev. Earth Planet. Sci. 2014.42:317-339. Downloaded from www.annualreviews.org
Access provided by Pennsylvania State University on 10/26/15. For personal use only.

Annu. Rev. Earth Planet. Sci. 2014.42:317-339. Downloaded from www.annualreviews.org
Access provided by Pennsylvania State University on 10/26/15. For personal use only.

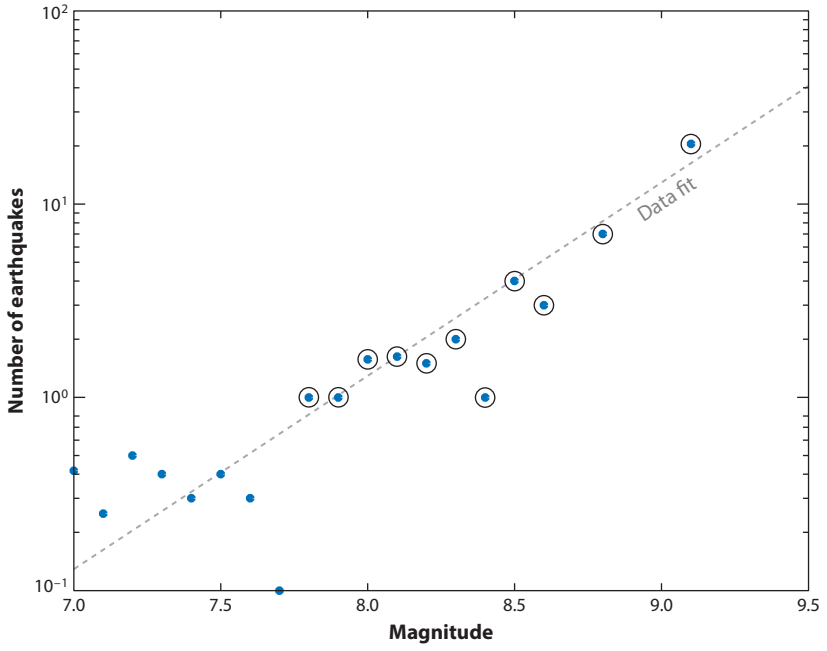

Figure 4

Number of earthquakes with magnitude ≥6 globally in 1 day following mainshocks of a given magnitude *M*. For the purpose of this plot, mainshocks are defined as earthquakes with no larger event within 4,500 km and 2 years prior. The circled points indicate aftershock numbers that are more than 1 standard deviation above the mean background rate and are therefore above the noise. The data are fit (*gray dashed line*) with the standard relationship of $N_{\text{aft}} = k10^M$, where N_{aft} is the number of aftershocks, *M* is the magnitude of the mainshock, and *k* is a fit parameter. Data span January 1, 1970, through December 31, 2013.

higher triggerability. Reprocessing the results of Velasco et al. (2008) shows this to be the case for triggered earthquakes detected as high-frequency bursts in seismograms from the Global Seismographic Network (**Figure 5**). The observed number of additional high-frequency bursts detected during the passage of the surface waves has a slightly higher than one-to-one scaling with the average rate.

APPLICATION 2: REGIONAL AND TEMPORAL VARIATIONS IN *f*

Globally, Pollitz et al. (2012) found a poor spatial correlation between seismic wave amplitude and the location of approximately 16 triggered sequences following the Sumatra–East Indian Ocean earthquakes of April 2012. Such a lack of correlation might be expected if there are real variations in triggerability due to tectonic regime and other factors. These variations carry information about the state of stress or strength of the crust.

Such variations in triggerability are observed at a large scale. Ordinary, tectonic earthquakes seem to be activated more often in shallow regions than deep, and only one clear example exists of dynamic triggering at more than 100 km depth on a subducting slab (Tibi et al. 2003). Extensional regions are more triggerable than compressional ones (Prejean & Hill 2009). For instance, most of crustal Japan has a relatively low incidence of triggering, but the southernmost island of Kyushu does have measureable dynamic triggering (Harrington & Brodsky 2006, van der Elst &

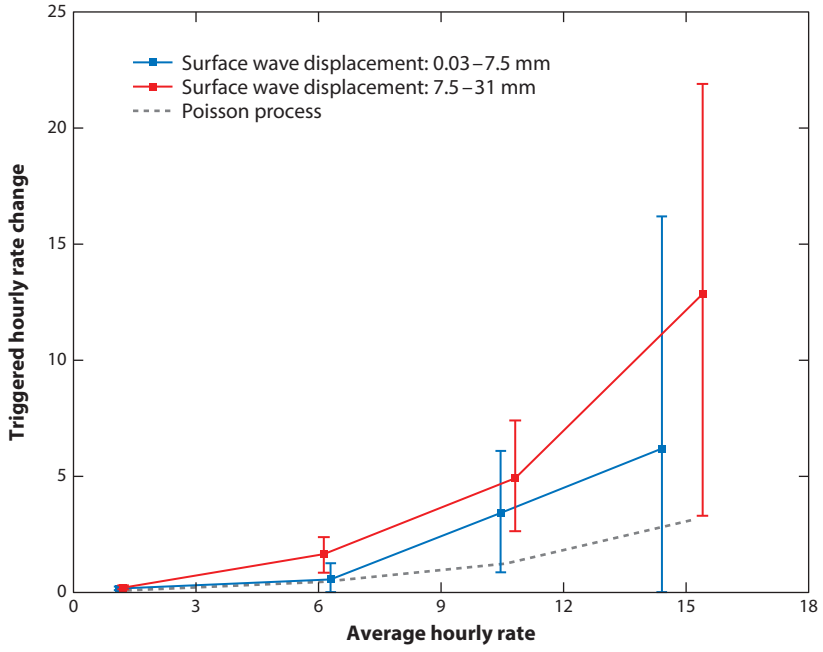

Figure 5

Rate change measured as the rate of excess events following the arrival of surface waves, from reprocessed 5-Hz high-pass filtered waveform data compiled by Velasco et al. (2008). The rate changes are therefore measured in a region centered on the station with a radius governed by the local detection capabilities in this frequency band (typically ~100 km for a magnitude 3 earthquake). The two curves with bootstrapped error bars represent the upper and lower 50% quantiles with respect to peak surface wave displacement (a proxy for dynamic strain). Both curves lie well above the 95% confidence bound for a Poisson process (*gray dashed line*). Rate change increases somewhat faster than linearly with average rate.

Brodsky 2010). This is the only part of Japan that is currently under extension. Compressional arcs might even occasionally show decreases in seismicity in response to seismic waves (Sánchez 2004). Another decrease in seismicity triggered by seismic waves was observed in a sequence of unusual, deep long-period events in Hawaii (Okubo & Wolfe 2008). These apparently dynamically triggered quiescences are an intriguing set of observations that are well worth following up in future studies. In any case, as a result of the variations between major tectonic regimes, a single global relationship between amplitude and triggering is not expected.

Triggerability also shows significant variations over the tens of kilometers scale (**Figure 6**). Geothermal areas in California have high triggerability, which is consistent with early observations that geothermal and volcanic areas had more reported instances of distant triggering (Hill et al. 1993). More interestingly, geothermal areas are not the only areas of high triggering. In particular, the northern end of the San Andreas creeping zone at the Calaveras fault in California is conspicuously high in triggerability.

High triggerability implies low f and therefore is a window into the in situ stress state. The exact interpretation depends on the mechanisms of triggering. However, any mechanism that ultimately results in frictional failure will have some dependence on the local fault strength. Fault strength can be low because pore pressure reduces the failure stress or because the local lithology has low friction.

Annu. Rev. Earth Planet. Sci. 2014.42:317-339. Downloaded from www.annualreviews.org
Access provided by Pennsylvania State University on 10/26/15. For personal use only.

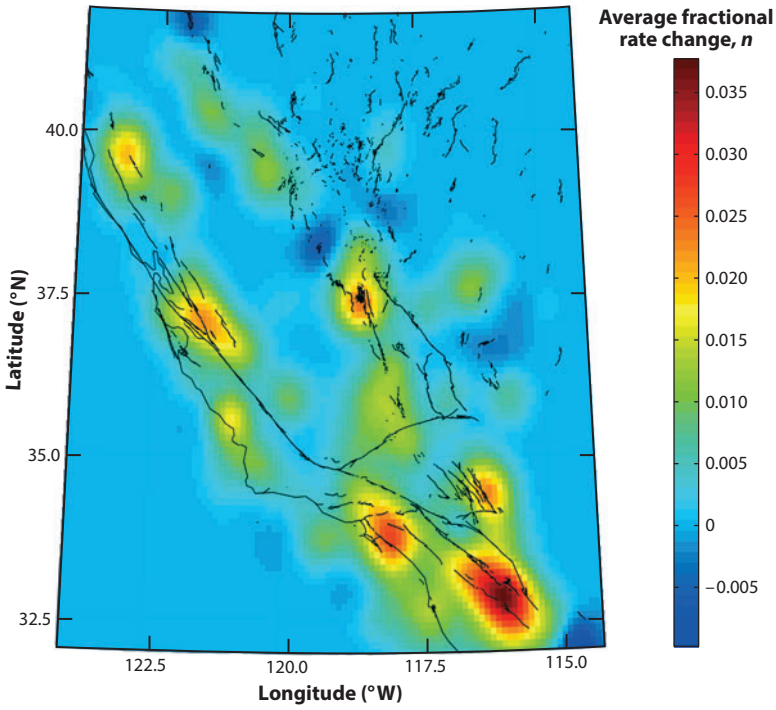

Figure 6

Remote triggering susceptibility in California. Colors correspond to average fractional rate change (Equation 3), measured in 0.1° spatial bins, for all potential remote triggering events with dynamic strain amplitude above 10^{-9}. Local earthquakes are drawn from the Advanced National Seismic System (ANSS) catalog for 1984–2009, with a magnitude cutoff of 2.1. Remote triggers are drawn from the global ANSS catalog of earthquakes greater than 800 km distant, for the same interval. Map is smoothed by a 0.3° Gaussian kernel. Modified from van der Elst & Brodsky (2010).

Observations of triggered tremor at the downdip locking limit in subduction zones and continental faults support this expectation. Triggered tremor has been observed at the transition region in Japan, Cascadia, and the downdip edge of the San Andreas (Miyazawa & Mori 2006, Peng et al. 2008, Rubinstein et al. 2007). These kinds of tremor are likely a composite signal from multiple, relatively low-rupture-velocity shear events (Shelly et al. 2006). The tremor observations lead to the conclusion that the conditions relevant to tremor also contribute to low *f*. This inference is also consistent with the extreme tidal sensitivity of tremor (Lambert et al. 2009; Nakata et al. 2008; Rubinstein et al. 2008; Thomas et al. 2009, 2012).

Some of the observations are consistent with large pore pressure playing a deciding role. In geothermal and volcanic fields, high fluid pressure and compartmentalization are likely to exist. A conspicuous exception to this interpretation is The Geysers geothermal field in northern California, which has one of the highest levels of triggerability recorded and only vaporstatic pressures in the field (Moore et al. 2000).

Outside of the plate boundary region, high triggerability in the United States is associated with areas of fluid injection and anthropogenic activity (van der Elst et al. 2013b). In these regions, heightened pore pressures reduce the effective stress and bring faults closer to failure. Again, low *f* corresponds to areas of pressurized, poorly drained fluids. This example in particular shows the power of dynamic triggering as a probe of the in situ stress state in the crust.

Annu. Rev. Earth Planet. Sci. 2014.42:317-339. Downloaded from www.annualreviews.org
Access provided by Pennsylvania State University on 10/26/15. For personal use only.

APPLICATION 3: PREDICTING EARTHQUAKES

If dynamic triggering follows well-defined laws as shown in **Figure 3**, then it should be possible to use it to predict future earthquake rate increases. Given observed ground motions, **Figure 3** predicts a specific, measureable quantity of earthquakes to follow. Of course, this method generally predicts very small earthquake rate increases for the distant events. The rate changes from even the largest distant earthquakes are approximately 10% of the background rate. In California, where the background rate averages on the order of one magnitude 2.1 or larger earthquake per day, the predicted triggered quantity of earthquakes is much less than one magnitude 2 earthquake per day for most distant earthquakes. This is clearly not a societally significant prediction.

However, the scaling in **Figure 3** is a scientifically useful prediction of future behavior that can be tested against prospective data. As shown above, the aftershock productivity is a function of the amplitude of the seismic waves. The statistical prediction is identical to that of an appropriately calibrated epidemic type aftershock sequence (ETAS) model that uses aftershock productivity combined with other statistical relationships to forecast earthquake rate (Ogata 1988, 2011). ETAS is one of the most successful operational forecasting methods currently available, but its connection to the underlying physics has been difficult to diagnose. The parameters of the model are entirely empirically determined from past history, and future studies would benefit from some connection to physical observables.

Although the function connecting wave amplitude and rate change is currently empirical, the dynamic triggering approach is a step forward in the sense that it is based on the amplitude of the seismic waves, which is a physical observable that can be measured with a sufficiently dense network of seismometers. This is a possible strategy to ultimately determine the physics behind the success of ETAS.

The above discussion is based on a regional average of triggerability. Certain areas provide particular sensitivity, and in these cases a societally useful prediction might be possible. Van der Elst et al. (2013b) found precursory triggering prior to moderate-magnitude, damaging induced earthquakes at fluid injection sites in the Midwestern United States. In these special circumstances, the presence of high triggerability might be a useful prediction of a future propensity toward moderate to large earthquakes.

A more far-reaching issue is the possibility of predicting extremely large earthquakes. In a retrospective study, van der Elst et al. (2013a) did not find precursory remote triggering prior to very large subduction zone earthquakes, but the study concluded that the catalogs had insufficient power to resolve small rate changes (~10%). Determining the importance of dynamic triggering in the world's most dangerous subduction zones will require seafloor instrumentation to improve the recording of small earthquakes offshore.

Societally relevant prediction requires information about magnitude as well as time and location of future earthquakes. The vast majority of recorded triggered earthquakes, like the vast majority of earthquakes in general, are small. As earthquakes normally follow a Gutenberg–Richter power law distribution in magnitude, large earthquakes are rare, so capturing their occurrence in a particular group of triggered earthquakes is difficult. On the one hand, Parsons & Velasco (2011) suggested that dynamically triggered earthquakes are limited to magnitudes less than 5, which they attribute to the paucity of available large faults oriented favorably over the many kilometers required for a large rupture (Parsons et al. 2012). On the other hand, Pollitz et al. (2012) documented a sequence of global dynamically triggered seismicity extending to magnitude 7, which suggests that the dynamic triggering of large events is a rare, but possible, scenario. The exact probability can be calculated by combining the triggering relationship of **Figure 3** with the Gutenberg–Richter distribution.

Annu. Rev. Earth Planet. Sci. 2014.42:317-339. Downloaded from www.annualreviews.org
Access provided by Pennsylvania State University on 10/26/15. For personal use only.

APPLICATION 4: EARTHQUAKE INITIATION PROCESSES

The early stages of an earthquake's growth are difficult to observe, yet critical to any hope of physically based earthquake prediction. Laboratory data on solid rock friction suggest that a well-defined nucleation phase should exist where accelerating creep in a small patch of a fault leads to runaway failure (Dieterich 1992). During the dynamic triggering events, this prediction is particularly testable as the forcing stress is known and the timing of failure can been followed. Other models, such as regional episodic creep or fault valving leading to a sudden change of pore pressure, should also have signatures in the triggering behavior.

Extracting information about the earthquake nucleation process requires a deeper understanding of triggering mechanisms. Up to this point we have been able to remain agnostic about the physical processes controlling dynamic triggering and its relation to *f*. We now embark on a review of plausible mechanisms and their relationships to the observations with an eye toward learning something about earthquake nucleation processes in general.

Mechanisms

Explanations for dynamic triggering have grappled with two basic observations: (1) the small amplitude of the perturbing stresses and (2) the common occurrence of delays between the perturbation and the resultant earthquakes. Both of these observations have been perplexing since the discovery of dynamic triggering (Hill et al. 1993).

The stress carried by the seismic waves is small compared with the ambient stress. For frictional failure, the shear stress required for failure is of the order of the lithostatic load, i.e., hundreds of megapascals at seismogenic depths. From **Figure 3**, the perturbing strains for resolvable triggered rates from distant earthquakes range from 3×10^{-9} to 2×10^{-7}. For a typical value of the shear modulus of rocks (3×10^{10} Pa), these strains correspond to shear stresses on the order of 10^{-4} to 10^{-2} MPa.

To some extent, the mystery of the apparent disproportionate impact of tiny stresses is resolved by the probabilistic view of *f*. In a large population of faults, there will always be a small fraction that are very close to failure, and rare triggering will occur for an arbitrarily small perturbation. The triggering signal requires either a large number of observations or an unusually large perturbing stress.

The delay of dynamic triggering is more problematic. Although some triggered events are in phase with the stress oscillations of the seismic waves, many others occur hours or days after the seismic waves have passed (Freed 2005, Hill & Prejean 2007). For instance, a majority of identifiable events in **Figure 2** occur in the hour after the end of the surface wave train from the mainshock. In some cases, the elevated seismicity does not appear to begin until hours or days after the end of the surface wave train. The prolonged nature of the triggering is one of the chief arguments for static stress changes rather than dynamic stresses as an agent for triggering earthquakes.

In addition to these two fundamental features, there are more detailed observations about dynamic triggering that arise from specific case studies that have mechanistic implications. These features include the propensity for triggering in extensional, hydrothermal, frictionally transitional, and anthropogenic regions (Hill & Prejean 2007). Another is the apparent preference for triggering by long-period waves within the seismic bandwidth (Brodsky & Prejean 2005). The efficacy of certain seismic waves or orientations in triggering also falls into this category (Hill 2008). Although all of these data are helpful, we consider their power in resolving mechanisms secondary to the two central features of dynamic triggering because the inferences all require observational confirmation and at this stage are based on a relatively small subset of the dynamic triggering cases.

Annu. Rev. Earth Planet. Sci. 2014.42:317-339. Downloaded from www.annualreviews.org
Access provided by Pennsylvania State University on 10/26/15. For personal use only.

A tertiary consideration in dynamic triggering mechanisms is consistency with nonseismic data sets. Seismic waves have been observed to trigger stream flow increases, spring discharge changes, groundwater head steps, creep events, and eruptions of magma, mud, or geysers (Elkhoury et al. 2006; Hammerschmidt et al. 2013; Hill et al. 1993, 1995; Johnson et al. 2001; Manga et al. 2012; Manga & Brodsky 2006; Roeloffs et al. 2003; Wang & Manga 2010; Wyatt et al. 1994). These triggered hydrological, geodetic, and volcanic processes are difficult to explain for exactly the same reasons as the seismicity; all are prolonged effects of transient, small stresses. It is tempting to devise a unified explanation for all of the teleseismic effects with a single mechanism. This might be an appropriate strategy, and some of the mechanisms below have this feature; however, it is not necessitated by the data.

Coulomb stress and local aftershocks. The most straightforward explanation of dynamic triggering is immediate, direct shear failure driven by the extra loading applied by the seismic waves. The combination of the additional shear stress of the elastic waves and the unloading from the fault normal components can push appropriately oriented faults over the Coulomb failure criteria.

In this framework, high pore pressures have often been invoked to explain the efficacy of small triggering stresses. For direct triggering by the seismic waves, reconciling the >2 orders of magnitude discrepancy between triggering stress amplitudes and the expected lithostatic load requires pore pressures that are $\gg$99% of lithostatic if faults are brought to failure from the beginning of their loading cycle. Extreme pore pressure elevation is possible in geothermal areas, which commonly have high triggerability. Such high pore pressure is also possible in the highly compartmentalized, hydrological structure of a fault zone. Such extreme conditions are not necessary if f is uniformly distributed and triggered earthquakes merely occur on those faults that happened to be late in the loading cycle.

Coulomb failure can explain why some faults fail at seismic wave stress amplitudes less than tidal stresses because it depends on fault orientation. Tidal stresses occur on a daily basis and might be expected to have already exhausted the faults extremely close to failure. However, tidal stresses are consistently applied with fixed orientations; the seismic waves apply a novel stress tensor that can preferentially load different fault orientations and result in new shear failures.

Coulomb failure by itself is an instantaneous response and therefore does not address delayed or prolonged triggering. However, once a triggered earthquake sequence is underway, local failure can occur through a cascade of aftershocks (Brodsky 2006). Each local earthquake triggers a sequence of other local earthquakes through a combination of static and dynamic stress interactions with local faults. If the triggered cascade follows the usual statistics of earthquake sequences, then significant triggering is expected from the small, often unobservable earthquakes in the sequence (Felzer et al. 2004, Helmstetter et al. 2005, Ogata 2004). This cascade may generate larger, observable earthquakes any time in the sequence. We refer to this explanation as the observationally delayed triggering model.

These unobserved cascades can trigger late, large earthquakes. As discussed before, each individual earthquake of magnitude M generates a number of aftershocks proportional to 10^M, and therefore the larger earthquakes are much more productive than the smaller ones (**Figure 4**). However, smaller earthquakes are much more abundant than larger ones. The usually observed Gutenberg–Richter relationship implies that the number of earthquakes of each magnitude is proportional to 10^{-bM}. Usually, $b = 1$ and these two effects therefore cancel each other out, and the total populations of earthquakes in every magnitude range are equally efficient in producing more events (Felzer et al. 2004, Helmstetter et al. 2005). Therefore, extremely small events that are undetectable by ordinary means can be effective in protracting a sequence and ultimately generating secondary aftershocks some time after the main event.

Annu. Rev. Earth Planet. Sci. 2014.42:317-339. Downloaded from www.annualreviews.org
Access provided by Pennsylvania State University on 10/26/15. For personal use only.

The observationally delayed triggering model makes some quantitative predictions. The case of having a secondary triggered earthquake that is larger than the directly triggered earthquakes reduces to the well-studied case of having an aftershock that is bigger than its mainshock (Felzer et al. 2004). The relative occurrence rate of these anomalously large aftershocks has been estimated on the basis of the ratio of observed foreshocks to aftershocks as ~25% (Brodsky 2011). This puts an upper bound on how commonly we should get observationally delayed triggering. Furthermore, the logarithmic decay of aftershock rates (Omori's law) means that the observational delay should be distributed uniformly over the logarithm of time. That is, there should be roughly as many episodes of triggering delayed by 1–10 days as are delayed by 0.1–1 days, and so on (Michael 2012). These predictions remain to be tested systematically against the dynamically triggered data sets.

In actuality, the earthquake sequence must have a lower magnitude limit in order to remain bounded (Sornette & Werner 2005). The extent of the sequence to very small earthquakes determines the overall productivity. Current observations suggest Gutenberg–Richter sequences can extend to magnitude −4, and therefore the cascade could potentially be very productive (Kwiatek et al. 2010).

Another test is a direct comparison of the productivity of the cascade with the productivity of the directly triggered events. This test for an extremely small group of earthquakes in The Geysers geothermal field showed that the productivity of the prolonged sequence was consistent with the cascade model (Brodsky 2006). Further studies of the statistics of triggered events and comparison with ordinary aftershock statistics would be useful contributions to the effort to untangle the mechanism of delayed triggering.

Alternatively, direct observation of the seismic waves of the small earthquakes during the delay time from sufficiently dense seismic networks could be attempted. Such waves may have been observed as the apparent nucleation phase of the triggered Nenana magnitude 3.7 event (Tape et al. 2013), but direct observation has proved elusive elsewhere. Instrumenting sufficiently densely for such observations is an important goal of future seismic deployments.

Despite the simplicity and many attractive qualities of the direct Coulomb failure/cascade hypothesis, problems do exist. Hill (2008) works through the stress orientations corresponding to various wavefields and fault orientations required to promote failure and concludes that direct triggering alone cannot easily explain the observations that (1) Rayleigh waves are more efficient at triggering than Love waves and (2) extensional regions are more triggerable than compressional ones. In addition, the geodetic, hydrological and other ancillary data sets are not readily explained by this model.

Rate-state friction. A useful extension of the Coulomb failure model is to incorporate a more nuanced form of the frictional failure criterion. Laboratory work has shown the frictional strength depends on the history of stressing as well as the current slip rate (Dieterich 1979, Ruina 1983; reviewed by Scholz 1998). In the experiments, an instantaneous change in slip rate on an interface from velocity v_0 to velocity v results in an instantaneous increase in friction that then relaxes to a steady state value. Rate-state friction is a parameterization of this behavior where the instantaneous increase in friction is fit by $a\ln(v/v_0)$ and the steady-state friction is fit with $(a - b)\ln(v/v_0)$, where a and b are empirical constants. If $b > a$, the frictional interface weakens with increasing velocity and therefore is unstable.

For an unstable fault, the transient increase in velocity during a seismic wave can reduce the friction, which further increases the slip velocity and leads to the failure, i.e., an earthquake. For large-amplitude waves or faults very near failure, the earthquake could happen immediately. For faults that are further from failure, the accelerating creep is prolonged and delayed triggering results.

Annu. Rev. Earth Planet. Sci. 2014.42:317-339. Downloaded from www.annualreviews.org
Access provided by Pennsylvania State University on 10/26/15. For personal use only.

Annu. Rev. Earth Planet. Sci. 2014.42:317-339. Downloaded from www.annualreviews.org
Access provided by Pennsylvania State University on 10/26/15. For personal use only.

While rate-state friction provides a mechanism for instantaneous and delayed triggering from transient deformation, it also introduces some caveats. Beeler & Lockner (2003) used laboratory and theoretical models to identify a critical timescale for nucleation that is a function of a, normal stress σ, and stressing rate. Stress oscillations with periods less than the frictional nucleation time should be less effective at driving precursory creep, because the high transient stressing rates result in high transient friction. This feedback between stressing rate and strength is not included in the simple Coulomb cartoon of **Figure 1**. They interpreted these results to explain the weak correlation of earthquakes with tidal stresses.[1] Because seismic waves are very short period compared with anticipated nucleation times, these feedback effects may limit the effectiveness of dynamic triggering via rate-state friction (Beeler & Lockner 2003). The inferred distribution of f is therefore most appropriately interpreted as stress required for failure at the frequency of seismic waves and may differ from the stress required for failure at lower stressing rates.

Dieterich (1994) combined rate-state friction equations with a specific distribution of stresses from failure to derive a constitutive law for seismicity. This semianalytical model provides the most ready comparison with dynamic triggering observations. Under the constitutive law, the rate change is again a function of the amplitude of the seismic waves relative to $a\sigma$. Large triggered earthquake rates therefore require low effective normal stress prior to the triggering. This is in contrast to the purely statistic interpretation of f discussed above. For example, applying the Dieterich (1994) model to the factor of 50 earthquake rate increase in Long Valley Caldera from the 2002 Denali earthquake requires extremely low effective stresses with pore pressures exceeding 99% of lithostatic (Brodsky & Prejean 2005).

An important shortcoming of rate-state triggering was pointed out by Gomberg (2001), concerning the duration of delayed triggering (see also the discussion in the review by Freed 2005). For any mechanism that invokes accelerating slip before failure, transient triggering will be most effective on faults late in their seismic cycles. Faults that are late in the cycle will be triggered instantaneously, and those that are loaded a little less will experience delayed triggering. However, the state dependence results in a peculiar effect: The further from failure a fault is, the less the triggering advances it toward failure (Gomberg 2001). This preferential advancement of the faults closest to failure implies that the duration of the triggered seismicity cannot exceed the duration of the transient. While rate-state friction can delay the onset of individual triggered earthquakes, it cannot by itself explain the prolonged triggered activity. An additional process is required to produce a prolonged rate increase.

The discussion so far has concerned advanced earthquakes, i.e., earthquakes that would have occurred eventually, even in the absence of triggering. A qualitatively different type of triggering can also occur because of rate-state friction. The full frictional law allows both creeping and locked behavior on faults. Therefore, earthquake triggering can also occur by driving a fault from the stable, creeping regime to the unstable, earthquake regime. This form of triggering is qualitatively different from the Coulomb failure discussed above, in which faults are advanced from a locked state to an earthquake. For the transition from stable to unstable sliding, the resultant earthquakes are not necessarily destined to fail in the absence of triggering.

The extra mode of triggering provides an explanation for the high triggerability of transitional zones between creeping and locked portions of faults. These transitional zones can occur because of either a change in the material properties or a change in effective normal stress along the fault (Rice & Ruina 1983). A change in effective normal stress or increase in fluid pressure can lead

[1]Note that more recent observations suggest that tidal stresses correlate better with earthquakes than originally thought (Cochran et al. 2004; Métivier et al. 2009; Tanaka 2010, 2012).

to stable sliding even on faults with intrinsically unstable rate dependence (Scholz 1998). These faults are called conditionally stable and should be particularly susceptible to seismic triggering by small-amplitude transients (Gomberg et al. 1998, Gu et al. 1984).

An additional factor contributing to high triggerability in the transitional zones is the link between frictional stability and stress drops in each earthquake. Both the stability and the stress drop depend on the difference between the low-velocity and high-velocity frictional stress of the fault (the quantity $a - b$). Near the stability transition, stress drop is low and faults reside closer to failure for their entire loading cycle (Scholz 2002). Therefore, they are expected to have relatively low values of f, as observed.

Viscous creep. Another variant on the direct triggering model is that the prolonged sequence is due to a local creep or slow slip event. This explanation has received increasing support with the proliferation of observations of slow slip phenomena in disparate settings (Peng & Gomberg 2010). Triggered slow slip has been proposed to explain sustained triggered tremor and low-frequency earthquakes along the deep San Andreas fault (Shelly et al. 2011). There is also evidence that such creep events drive the migration of aftershocks and earthquake swarms (Lohman & McGuire 2007, Peng & Zhao 2009). A few observations of triggered deformation support the hypothesis, including a geodetically observed interplate slow slip event that was triggered by teleseismic surface waves in southwest Japan (Hill et al. 1995, Itaba & Ando 2011, Wyatt et al. 1994). In at least one case, an increasing-amplitude tremor-like signal was observed to temporally connect the arrival of a triggering wave with the eventual occurrence of a triggered earthquake (Tape et al. 2013).The mechanism for initiating the creep is unclear and requires either time-dependent frictional properties that are fatigued by the transient wave or a migration of fluid pressure (see below).

Permeability enhancement. Most of the macroscopic observations related to distant earthquakes are hydrological. Stream flows can increase, tidal responses can change, and water levels in open wells can suddenly shift (Brodsky et al. 2003, Elkhoury et al. 2006, Manga et al. 2003, Wang & Manga 2010). As fluid movement and pore pressure changes are some of the best-understood ways to trigger earthquakes in well-understood artificial situations, it seems useful to seek a unified explanation for all these macroscopic effects of the small stress in seismic waves.

A growing body of evidence suggests that the hydrological effects in the far field are due to permeability enhancement. The clearest examples come from tidal responses, which separate head changes from transport properties. At a key site in Piñon Flats, California, the permeability enhancement coincides with regional earthquakes and increases with the amplitude of the seismic waves (**Figure 7**) (Elkhoury et al. 2006). This behavior mimics the rate changes of dynamic triggering and is reproducible in laboratory experiments (**Figure 8**) (Elkhoury et al. 2011). The permeability enhancements are attributable to the large flow driven by the seismic waves unclogging fractures and removing temporary barriers, like those developed during healing and sealing of veins in the fault zone. Recently, Xue et al. (2013) observed permeability enhancement associated with distant earthquakes inside the fault zone that generated the M_w 7.9 2008 Wenchuan earthquake. Note that the high storage contrast of fault systems at depth results in a large flow resulting from a very small stress in the waves. This inherent amplification effect in the hydrogeology is an important part of the apparent efficacy of the process.

The increased permeability can trigger earthquakes through two distinct mechanisms: drainage or pore pressure redistribution. As noted by Segall & Rice (1995), the drainage state is important for the slip stability of a gouge-filled fault. A sudden increase in permeability can reduce the suction force related to fault zone dilation, thus releasing the brakes on seismic slip. This potential connection between drainage state and fault stability helps explain the high triggerability at transitional

Annu. Rev. Earth Planet. Sci. 2014.42:317-339. Downloaded from www.annualreviews.org
Access provided by Pennsylvania State University on 10/26/15. For personal use only.

Annu. Rev. Earth Planet. Sci. 2014.42:317-339. Downloaded from www.annualreviews.org
Access provided by Pennsylvania State University on 10/26/15. For personal use only.

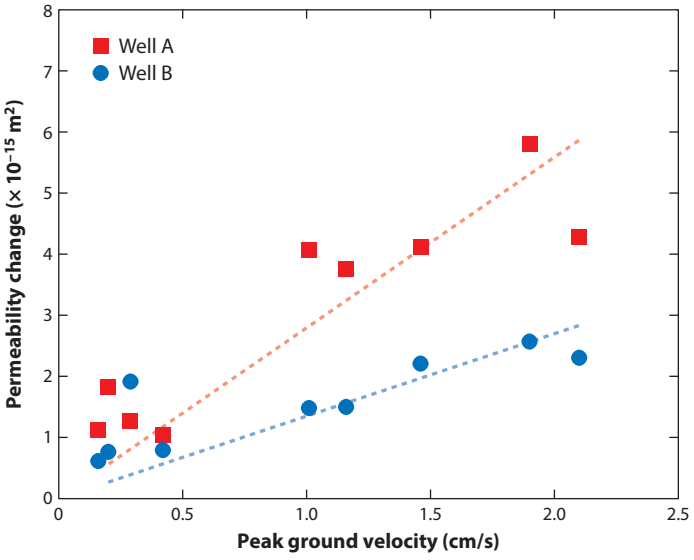

Figure 7

Permeability change measured through tidal response in shallow water wells as a function of local peak ground velocity in the seismic waves from regional earthquakes. Each color denotes a separate well at the site. Modified from Elkhoury et al. (2006).

regions, as discussed in Application 2 above. The drainage mechanism is also useful in explaining the high triggerability of The Geysers geothermal field, which has low pore pressure but abundant precipitation, creating potentially fragile permeability structures in the hydrothermal system.

In addition, permeability enhancement can promote earthquakes through simply changing the strength in locked portions of the fault. Permeability enhancement allows fluid flow from high- to low-pressure regions. The breached, high-pressure patches remain quiescent, while the effective stress is reduced in the regions inundated by high pressure. These weakened patches of the fault therefore can fail and generate earthquakes (Brodsky & Prejean 2005).

Granular flow. Another set of proposed mechanisms for triggering involves granular flow. The ubiquitous gouge in fault zones results in a complex rheology that can be particularly sensitive to vibrations because of the stress heterogeneity in the grain pack. For instance, acoustic waves can result in weakening, and the loss of strength could potentially nucleate an earthquake (Johnson et al. 2008, Melosh 1979, van der Elst et al. 2012). In a granular system, a large portion of the load is supported by localized force chains, and individual grains support a large-tailed distribution of stresses (Jaeger et al. 1996). As a result, many grains are held in contact by relatively small normal stress and have correspondingly weak frictional locking (Aharonov & Sparks 2002). These weak networks may be extremely important for the buckling strength of the strong force chain networks (Tordesillas & Muthuswamy 2009). This allows a small perturbation to potentially have a major effect.

Granular flow mechanisms require relatively low effective confining stress to operate, as the basic locking mechanism is still frictional contacts between grains (van der Elst et al. 2012). If confining stresses are indeed this low, then this variant of frictional instability is nearly identical in its predictions to the direct Coulomb or rate-state failure criteria. The only significant difference is that the grain pack may have a different sensitivity to the orientation of the stress tensor than

Annu. Rev. Earth Planet. Sci. 2014.42:317-339. Downloaded from www.annualreviews.org
Access provided by Pennsylvania State University on 10/26/15. For personal use only.

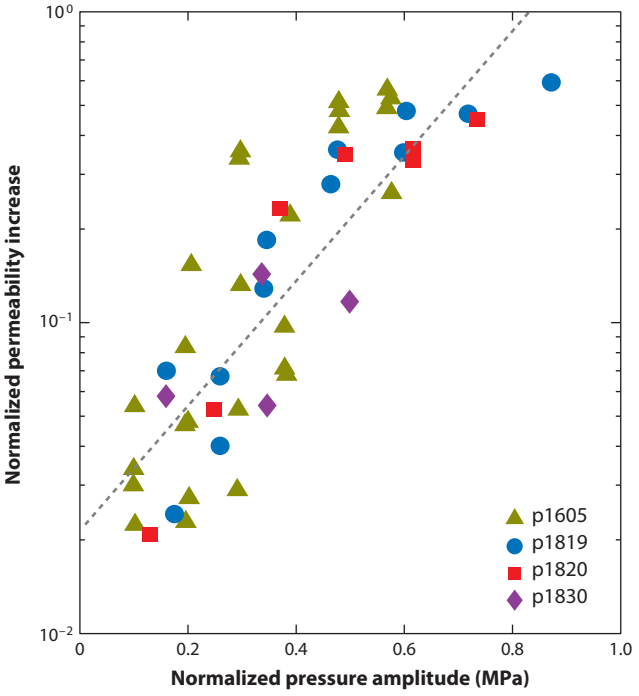

Figure 8

Experimentally produced permeability increases generated by oscillating the pore pressure in a fractured rock under high confining pressure. As dilatational strain of the waves generates pore pressure oscillations, these experiments demonstrate that transient elastic waves can produce persistent permeability changes. Permeability increases are normalized by the initial permeability for each sample and therefore unitless. Symbol key codes correspond to individual experiments from the Penn State laboratory. Modified from Elkhoury et al. (2011).

do the solid surfaces. Dilatational strains (acoustic waves) can be very effective at weakening a granular medium. This fact agrees with the observation that Rayleigh waves are more effective at triggering earthquakes than Love waves.

Subcritical crack growth. Seismic waves can fatigue cracks and generate subcritical growth. Normally, cracks only grow once they reach a critical length at which the elastic energy release from further lengthening exceeds the energy expenditure of creating a new surface. However, hot fluids at crack tips can facilitate chemical reactions that allow the stress concentration to break bonds and result in crack growth (Atkinson 1984). This subcritical crack growth is further assisted by the ratcheting effect of seismic waves. Again, the stress orientations possible are diverse. The only requirement is availability of elevated fluid temperature and pressures.

Laboratory data on rates of subcritical crack growth are limited. The general functional forms of the predictions are similar to those for rate-state friction (Brodsky & Prejean 2005, Kanamori & Brodsky 2004). In order to fully assess this possibility, more laboratory data are needed.

Obsolete mechanisms. Some proposed mechanisms for triggered seismicity have been shown to be ineffective on the basis of the current set of observations and improved theoretical understanding. Early work on dynamic triggering invoked bubble dynamics based on the understanding that

dynamic triggering was prevalent in volcanic and geothermal areas. Specifically, studies invoked rectified diffusion in which the seismic waves pumped gas into bubbles to result in an increase in pressure and advective overpressure in which rising, high-pressure bubbles from the bottom of a magma chamber carried their high-pressure state to upper levels (Brodsky et al. 1998, Linde et al. 1994, Sturtevant et al. 1996). Because dynamic triggering is now understood to be a more widespread phenomenon, such restricted mechanisms are not appropriate everywhere. Furthermore, the early bubble pressurization theories underappreciated the effect of pressure increases on changing the solubility of gas species. More complete treatments have shown that bubbles tend to resorb before the pressurization due to rectified diffusion or advective overpressure becomes significant (Ichihara & Brodsky 2006).

Implications for Nucleation

Given the above considerations and observations, we have learned that dynamic triggering probably requires a sequence of mechanisms. The relative insensitivity to radiation pattern and the dominant effect of the Rayleigh wave both suggest a complex process that is not directly propelling shear surfaces to failure in a well-defined orientation. Most data can be explained by Coulomb failure with rate-state friction followed by either aseismic creep or a cascade of earthquakes to generate the prolonged effect. Permeability enhancement leading to drainage or pore pressure redistribution on faults is also a possibility, with the added attraction that it addresses the nonseismological far-field hydrologic observations.

From the dynamic triggering constraints, we can extrapolate that earthquake initiation in general may be a multistage process. At least one prolonging process should be active in fault zones regardless of the origin of the mainshock nucleation process. Aseismic creep and/or triggering cascades with a perpetual stressing must be an important part of controlling earthquake timing in addition to any direct frictional failure effects. If the permeability enhancement mechanisms ultimately prove to be correct, understanding the hydrogeological coupling of faults will prove to be an important goal of earthquake physics.

Importantly, the statistical interpretation of the failure stresses means that dynamic triggering mechanisms can operate at high effective stress (low pore pressure) because a distribution of loading and stresses in the crust allows the subset of faults near failure to be triggered, regardless of mean stress. However, the regional variations in triggerability that correlate with areas known to have active geothermal systems suggest a role for fluids. Furthermore, if the constitutive law for seismicity in the widely used Dieterich (1994) model is correct, low effective stresses are required to explain the magnitude of the observed relative rate changes. If such a specific constitutive law is not appropriate, then low effective stress is not necessary.

Ultimately, discrimination between the mechanisms will rely on determining whether or not the ancillary data sets such as permeability enhancement and geodetic transients are related to the earthquake triggering processes. Finding data sets that connect the multiple types of data will be key. Time-dependent seismic velocity measurements, active sampling of fault zones, and borehole observations close to the hypocenters of the triggered events are all possible strategies. Taira et al. (2009) demonstrated that scatterers in the fault zone change in reaction to distant earthquakes, and they connected this observation with changes in local earthquake recurrence time. This study is exemplary of the type needed to put these pieces together.

CONCLUSIONS

Dynamic triggering has matured. The phenomenon is well established and can be used as a tool to address other problems in earthquake physics. Although the mechanisms of dynamic triggering

Annu. Rev. Earth Planet. Sci. 2014.42:317-339. Downloaded from www.annualreviews.org
Access provided by Pennsylvania State University on 10/26/15. For personal use only.

are still unclear, the observations show that the seismicity rate changes are well-defined functions of the perturbing stresses.

From this basic insight, we have learned that the distribution of stress from failure is uniform in California, which in turn suggests that faults are uniformly distributed over their loading cycles. Some regional variations in triggerability have been documented. The propensity for extensional, frictionally transitional, and anthropogenic seismicity areas to be triggered provides a probe of the failure process in all of these regions. Dynamic triggering can be used to elucidate the physics behind statistical earthquake predictions by connecting the rate changes to the observable amplitude of the seismic waves. Ultimately, dynamic triggering predictions may be as useful as any other operational statistical forecast method.

Finally, we have learned from dynamic triggering that a multistage earthquake initiation process is likely. The data invite multidisciplinary studies to connect the hydrogeological, frictional, geodetic, geological, and seismological evidence together to uncover the ways in which one earthquake leads to another.

Annu. Rev. Earth Planet. Sci. 2014.42:317-339. Downloaded from www.annualreviews.org
Access provided by Pennsylvania State University on 10/26/15. For personal use only.

DISCLOSURE STATEMENT

The authors are not aware of any affiliations, memberships, funding, or financial holdings that might be perceived as affecting the objectivity of this review.

ACKNOWLEDGMENTS

We thank R. Bürgmann, T. Lay, S. Prejean, and H. Savage for helpful comments on the manuscript.

LITERATURE CITED

Aharonov E, Sparks D. 2002. Shear profiles and localization in simulations of granular materials. *Phys. Rev. E* 65:051302

Aiken C, Peng Z, Chao K. 2013. Tremors along the Queen Charlotte Margin triggered by large teleseismic earthquakes. *Geophys. Res. Lett.* 40:829–34

Atkinson BK. 1984. Subcritical crack growth in geological materials. *J. Geophys. Res.* 89:4077–114

Beeler NM, Lockner DA. 2003. Why earthquakes correlate weakly with the solid Earth tides: effects of periodic stress on the rate and probability of earthquake occurrence. *J. Geophys. Res.* 108(B8):2391

Brodsky EE. 2006. Long-range triggered earthquakes that continue after the wave train passes. *Geophys. Res. Lett.* 33:L15313

Brodsky EE. 2011. The spatial density of foreshocks. *Geophys. Res. Lett.* 38:L10305

Brodsky EE, Prejean S. 2005. New constraints on mechanisms of remotely triggered seismicity at Long Valley Caldera. *J. Geophys. Res.* 110:B04302

Brodsky EE, Roeloffs E, Woodcock D, Gall I, Manga M. 2003. A mechanism for sustained groundwater pressure changes induced by distant earthquakes. *J. Geophys. Res.* 108(B8):2390

Brodsky EE, Sturtevant B, Kanamori H. 1998. Earthquakes, volcanoes, and rectified diffusion. *J. Geophys. Res.* 103(B10):23827–38

Cochran ES, Vidale JE, Tanaka S. 2004. Earth tides can trigger shallow thrust fault earthquakes. *Science* 306:1164–66

Dieterich JH. 1979. Modeling of rock friction: 1. Experimental results and constitutive equations. *J. Geophys. Res.* 84:2161

Dieterich JH. 1992. Earthquake nucleation on faults with rate- and state-dependent strength. *Tectonophysics* 211:115–34

Dieterich JH. 1994. A constitutive law for rate of earthquake production and its application to earthquake clustering. *J. Geophys. Res.* 99(B2):2601–18
Elkhoury JE, Brodsky EE, Agnew DC. 2006. Seismic waves increase permeability. *Nature* 441:1135–38
Elkhoury JE, Niemeijer A, Brodsky EE, Marone C. 2011. Laboratory observations of permeability enhancement by fluid pressure oscillation of in situ fractured rock. *J. Geophys. Res.* 116:B02311
Felzer KR, Abercrombie R, Ekström G. 2004. A common origin for aftershocks, foreshocks, and multiplets. *Bull. Seismol. Soc. Am.* 94:88
Felzer KR, Brodsky EE. 2005. Testing the stress shadow hypothesis. *J. Geophys. Res.* 110:B05S09
Felzer KR, Brodsky EE. 2006. Decay of aftershock density with distance indicates triggering by dynamic stress. *Nature* 441:735–38
Freed AM. 2005. Earthquake triggering by static, dynamic, and postseismic stress transfer. *Annu. Rev. Earth Planet. Sci.* 33:335–367
Frohlich C, Davis S. 1985. Identification of aftershocks of deep earthquakes by a new ratios method. *Geophys. Res. Lett.* 12:713–16
Gomberg J. 2001. The failure of earthquake failure models. *J. Geophys. Res.* 106(B8):16253–63
Gomberg J, Beeler NM, Blanpied ML, Bodin P. 1998. Earthquake triggering by transient and static deformations. *J. Geophys. Res.* 103(B10):24411–26
Gomberg J, Bodin P, Larson K, Dragert H. 2004. Earthquake nucleation by transient deformations caused by the $M = 7.9$ Denali, Alaska, earthquake. *Nature* 427:621–24
Gomberg J, Davis S. 1996. Stress/strain changes and triggered seismicity at The Geysers, California. *J. Geophys. Res.* 101(B1):733–49
Gomberg J, Felzer K. 2008. A model of earthquake triggering probabilities and application to dynamic deformations constrained by ground motion observations. *J. Geophys. Res.* 113:B10317
Gomberg J, Reasenberg P, Bodin P, Harris R. 2001. Earthquake triggering by seismic waves following the Landers and Hector Mine earthquakes. *Nature* 411:462–66
Gu J-C, Rice JR, Ruina AL, Tse ST. 1984. Slip motion and stability of a single degree of freedom elastic system with rate and state dependent friction. *J. Mech. Phys. Solids* 32:167–96
Hammerschmidt S, Davis EE, Kopf A. 2013. Fluid pressure and temperature transients detected at the Nankai Trough Megasplay Fault: results from the SmartPlug borehole observatory. *Tectonophysics* 600:116–33
Harrington RM, Brodsky EE. 2006. The absence of remotely triggered seismicity in Japan. *Bull. Seismol. Soc. Am.* 96:871–78
Helmstetter A, Kagan Y, Jackson D. 2005. Importance of small earthquakes for stress transfers and earthquake triggering. *J. Geophys. Res.* 110:B05S08
Hill DP. 2008. Dynamic stresses, Coulomb failure, and remote triggering. *Bull. Seismol. Soc. Am.* 98:66–92
Hill DP, Johnston MJ, Langbein JO, Bilham R. 1995. Response of Long Valley caldera to the $M_w = 7.3$ Landers, California, earthquake. *J. Geophys. Res.* 100(B7):12985–3005
Hill DP, Prejean SG. 2007. Dynamic triggering. In *Earthquake Seismology*, ed. H Kanamori, pp. 257–91. Treatise Geophys. 4. Amsterdam: Elsevier
Hill DP, Reasenberg PA, Michael A, Arabaz WJ, Beroza G, et al. 1993. Seismicity remotely triggered by the magnitude 7.3 Landers, California, earthquake. *Science* 260:1617–23
Ichihara M, Brodsky EE. 2006. A limit on the effect of rectified diffusion in volcanic systems. *Geophys. Res. Lett.* 33:L02316
Itaba S, Ando R. 2011. A slow slip event triggered by teleseismic surface waves. *Geophys. Res. Lett.* 38:L21306
Jaeger HM, Nagel SR, Behringer RP. 1996. Granular solids, liquids, and gases. *Rev. Mod. Phys.* 68:1259–73
Johnson HP, Dziak RP, Fisher CR, Fox CG, Pruis MJ. 2001. Earthquakes' impact on hydrothermal systems may be far-reaching. *Eos Trans. AGU* 82:233–36
Johnson PA, Savage H, Knuth M, Gomberg J, Marone C. 2008. Effects of acoustic waves on stick-slip in granular media and implications for earthquakes. *Nature* 451:57–60
Kanamori H, Brodsky EE. 2001. The physics of earthquakes. *Phys. Today* 54:34
Kanamori H, Brodsky EE. 2004. The physics of earthquakes. *Rep. Prog. Phys.* 67:1429
Kwiatek G, Plenkers K, Nakatani M, Yabe Y. 2010. Frequency-magnitude characteristics down to magnitude-4.4 for induced seismicity recorded at Mponeng Gold Mine, South Africa. *Bull. Seismol. Soc. Am.* 100:1165–73

Annu. Rev. Earth Planet. Sci. 2014.42:317-339. Downloaded from www.annualreviews.org
Access provided by Pennsylvania State University on 10/26/15. For personal use only.

Lambert A, Kao H, Rogers G, Courtier N. 2009. Correlation of tremor activity with tidal stress in the northern Cascadia subduction zone. *J. Geophys. Res.* 114:B00A08
Linde AT, Sacks IS, Johnston MJS, Hill DP, Bilham RG. 1994. Increased pressure from rising bubbles as a mechanism for remotely triggered seismicity. *Nature* 371:408–10
Lohman RB, McGuire JJ. 2007. Earthquake swarms driven by aseismic creep in the Salton Trough, California. *J. Geophys. Res.* 112:B04405
Manga M, Beresnev I, Brodsky EE, Elkhoury JE, Elsworth D, et al. 2012. Changes in permeability caused by transient stresses: field observations, experiments, and mechanisms. *Rev. Geophys.* 50:RG2004
Manga M, Brodsky E. 2006. Seismic triggering of eruptions in the far field: volcanoes and geysers. *Annu. Rev. Earth Planet. Sci.* 34:263–91
Manga M, Brodsky E, Boone M. 2003. Response of streamflow to multiple earthquakes. *Geophys. Res. Lett.* 30:1214
Melosh HJ. 1979. Acoustic fluidization: a new geologic process? *J. Geophys. Res.* 84(B13):7513–20
Métivier L, de Viron O, Conrad CP, Renault S, Diament M, Patau G. 2009 Evidence of earthquake triggering by the solid Earth tides. *Earth Planet. Sci. Lett.* 278:370–75
Michael AJ. 2012. Do aftershock probabilities decay with time? *Seismol. Res. Lett.* 83:630–32
Miyazawa M, Mori J. 2006. Evidence suggesting fluid flow beneath Japan due to periodic seismic triggering from the 2004 Sumatra-Andaman earthquake. *Geophys. Res. Lett.* 33:5303
Moore JN, Adams MC, Anderson AJ. 2000. The fluid inclusion and mineralogic record of the transition from liquid- to vapor-dominated conditions in The Geysers geothermal system, California. *Econ. Geol.* 95:1719–37
Nakata R, Suda N, Tsuroka H. 2008. Non-volcanic tremor resulting from the combined effect of Earth tides and slow slip events. *Nat. Geosci.* 1:676–78
Ogata Y. 1988. Statistical models for earthquake occurrences and residual analysis for point processes. *J. Am. Stat. Assoc.* 83:9–27
Ogata Y. 2004. Space-time model for regional seismicity and detection of crustal stress changes. *J. Geophys. Res.* 109:B03308
Ogata Y. 2011. Significant improvements of the space-time ETAS model for forecasting of accurate baseline seismicity. *Earth Planets Space* 63:217–29
Okubo PG, Wolfe CJ. 2008. Swarms of similar long-period earthquakes in the mantle beneath Mauna Loa Volcano. *J. Volcanol. Geotherm. Res.* 178:787–94
Parsons T, Kaven JO, Velasco AA, Gonzales-Huizar H. 2012. Unraveling the apparent magnitude threshold of remote earthquake triggering using full wavefield surface wave simulation. *Geochem. Geophys. Geosyst.* 13:Q06016
Parsons T, Velasco AA. 2011. Absence of remotely triggered large earthquakes beyond the mainshock region. *Nat. Geosci.* 4:312–16
Peng Z, Gomberg J. 2010. An integrated perspective of the continuum between earthquakes and slow-slip phenomena. *Nat. Geosci.* 3:599–607
Peng Z, Vidale JE, Creager KC, Rubinstein JL, Gomberg J, Bodin P. 2008. Strong tremor near Parkfield, CA, excited by the 2002 Denali Fault earthquake. *Geophys. Res. Lett.* 35:L23305
Peng Z, Zhao P. 2009. Migration of early aftershocks following the 2004 Parkfield earthquake. *Nat. Geosci.* 2:877–81
Pollitz FF, Stein RS, Sevilgen V, Bürgmann R. 2012. The 11 April 2012 east Indian Ocean earthquake triggered large aftershocks worldwide. *Nature* 490:250–53
Prejean SG, Hill DP. 2009. Dynamic triggering of earthquakes. In *Encyclopedia of Complexity and Systems Science*, ed. R Meyers, pp. 2600–621. New York: Springer
Raleigh CB, Healy JH, Bredehoeft JD. 1976. Experiment in earthquake control at Rangely, Colorado. *Science* 191:1230–37
Reasenberg PA, Jones LM. 1990. California aftershock hazard forecasts. *Science* 247:345–46
Reid HF. 1911. The elastic-rebound theory of earthquakes. *Univ. Calif. Publ. Bull. Dep. Geol.* 6:413–44
Rice JR, Ruina AL. 1983. Stability of steady frictional slipping. *J. Appl. Mech.* 50:343–49
Roeloffs E, Sneed M, Galloway D, Sorey M, Farrar C, et al. 2003. Water-level changes induced by local and distant earthquakes at Long Valley caldera, California. *J. Volcanol. Geotherm. Res.* 127:269–303

Annu. Rev. Earth Planet. Sci. 2014.42:317-339. Downloaded from www.annualreviews.org
Access provided by Pennsylvania State University on 10/26/15. For personal use only.

Rubinstein JL, La Rocca M, Vidale JE, Creager KC, Wech AG. 2008. Tidal modulation of nonvolcanic tremor. *Science* 319:186

Rubinstein JL, Vidale JE, Gomberg J, Bodin P, Creager KC, Malone SD. 2007. Non-volcanic tremor driven by large transient shear stresses. *Nature* 448:579–82

Ruina A. 1983. Slip instability and state variable friction laws. *J. Geophys. Res.* 88(B12):10359–70

Sánchez JJ. 2004. Intermediate-term declines in seismicity at Mt. Wrangell and Mt. Veniaminof volcanoes, Alaska, following the 3 November 2002 M_w 7.9 Denali fault earthquake. *Bull. Seismol. Soc. Am.* 94:S370–83

Scholz CH. 1998. Earthquakes and friction laws. *Nature* 391:37–42

Scholz CH. 2002. *Mechanics of Earthquakes and Faulting*. Cambridge, UK: Cambridge Univ. Press.

Segall P, Rice JR. 1995. Dilatancy, compaction, and slip instability of a fluid-infiltrated fault. *J. Geophys. Res.* 100(B11):22155–71

Shelly DR, Beroza GC, Ide S, Nakamula S. 2006. Low-frequency earthquakes in Shikoku, Japan, and their relationship to episodic tremor and slip. *Nature* 442:188–91

Shelly DR, Peng Z, Hill DP, Aiken C. 2011. Triggered creep as a possible mechanism for delayed dynamic triggering of tremor and earthquakes. *Nat. Geosci.* 4:384–88

Sornette D, Werner MJ. 2005. Constraints on the size of the smallest triggering earthquake from the epidemic-type aftershock sequence model, Båth's law, and observed aftershock sequences. *J. Geophys. Res.* 110:B08304

Stroup DF, Bohnenstiehl DR, Tolstoy M, Waldhauser F, Weekly RT. 2007. Pulse of the seafloor: tidal triggering of microearthquakes at 9°50′N East Pacific Rise. *Geophys. Res. Lett.* 34:L15301

Sturtevant B, Kanamori H, Brodsky EE. 1996. Seismic triggering by rectified diffusion in geothermal systems. *J. Geophys. Res.* 101(B11):25269–82

Taira T, Silver PG, Niu F, Nadeau RM. 2009. Remote triggering of fault-strength changes on the San Andreas fault at Parkfield. *Nature* 461:636–39

Tanaka S. 2010. Tidal triggering of earthquakes precursory to the recent Sumatra megathrust earthquakes of 26 December 2004 (M_w 9.0), 28 March 2005 (M_w 8.6), and 12 September 2007 (M_w 8.5). *Geophys. Res. Lett.* 37:L02301

Tanaka S. 2012. Tidal triggering of earthquakes prior to the 2011 Tohoku-Oki earthquake (M_w 9.1). *Geophys. Res. Lett.* 39:L00G26

Tape C, West M, Silwal V, Ruppert N. 2013. Earthquake nucleation and triggering on an optimally oriented fault. *Earth Planet. Sci. Lett.* 363:231–41

Thomas AM, Bürgmann R, Shelly DR, Beeler NM, Rudolph ML. 2012. Tidal triggering of low frequency earthquakes near Parkfield, California: implications for fault mechanics within the brittle-ductile transition. *J. Geophys. Res.* 117:B05301

Thomas AM, Nadeau RM, Bürgmann R. 2009. Tremor-tide correlations and near-lithostatic pore pressure on the deep San Andreas fault. *Nature* 462:1048–51

Tibi R, Wiens DA, Inoue H. 2003. Remote triggering of deep earthquakes in the 2002 Tonga sequences. *Nature* 424:921–25

Tordesillas A, Muthuswamy M. 2009. On the modeling of confined buckling of force chains. *J. Mech. Phys. Solids* 57:706–27

Townend J, Zoback MD. 2000. How faulting keeps the crust strong. *Geology* 28:399–402

van der Elst N, Brodsky EE. 2010. Connecting near-field and far-field earthquake triggering to dynamic strain. *J. Geophys. Res.* 115:B07311

van der Elst NJ, Brodsky EE, Lay T. 2013a. Remote triggering not evident near epicenters of impending great earthquakes. *Bull. Seismol. Soc. Am.* 103:1522–40

van der Elst NJ, Brodsky EE, Le Bas P-Y, Johnson PA. 2012. Auto-acoustic compaction in steady shear flows: experimental evidence for suppression of shear dilatancy by internal acoustic vibration. *J. Geophys. Res.* 117:B09314

van der Elst NJ, Savage HM, Keranen KM, Abers GA. 2013b. Enhanced remote earthquake triggering at fluid-injection sites in the midwestern United States. *Science* 341:164–67

Velasco AA, Hernandez S, Parsons T, Pankow K. 2008. Global ubiquity of dynamic earthquake triggering. *Nat. Geosci.* 1:375–79

Annu. Rev. Earth Planet. Sci. 2014.42:317-339. Downloaded from www.annualreviews.org
Access provided by Pennsylvania State University on 10/26/15. For personal use only.

Wang C-Y, Manga M. 2010. *Earthquakes and Water*. New York: Springer-Verlag
West M, Sánchez JJ, McNutt SR. 2005. Periodically triggered seismicity at Mount Wrangell, Alaska, after the Sumatra earthquake. *Science* 308:1144–46
Wu C, Peng Z, Wang W, Chen Q-F. 2011. Dynamic triggering of shallow earthquakes near Beijing, China. *Geophys. J. Int.* 185:1321–34
Wyatt FK, Agnew DC, Gladwin M. 1994. Continuous measurements of crustal deformation for the 1992 Landers earthquake sequence. *Bull. Seismol. Soc. Am.* 84:768–79
Xue L, Li HB, Brodsky EE, Xu ZQ, Kano Y, et al. 2013. Continuous permeability measurements record healing inside the Wenchuan earthquake fault zone. *Science* 340:1555–59

Annu. Rev. Earth Planet. Sci. 2014.42:317-339. Downloaded from www.annualreviews.org
Access provided by Pennsylvania State University on 10/26/15. For personal use only.

Annual Review
of Earth and
Planetary Sciences
Volume 42, 2014

Contents

Falling in Love with Waves
Hiroo Kanamori 1

The Diversity of Large Earthquakes and Its Implications for Hazard Mitigation
Hiroo Kanamori 7

Broadband Ocean-Bottom Seismology
Daisuke Suetsugu and Hajime Shiobara 27

Extrasolar Cosmochemistry
M. Jura and E.D. Young 45

Orbital Climate Cycles in the Fossil Record: From Semidiurnal to Million-Year Biotic Responses
Francisco J. Rodríguez-Tovar 69

Heterogeneity and Anisotropy of Earth's Inner Core
Arwen Deuss 103

Detrital Zircon U-Pb Geochronology Applied to Tectonics
George Gehrels 127

How Did Early Earth Become Our Modern World?
Richard W. Carlson, Edward Garnero, T. Mark Harrison, Jie Li, Michael Manga, William F. McDonough, Sujoy Mukhopadhyay, Barbara Romanowicz, David Rubie, Quentin Williams, and Shijie Zhong 151

The Stardust Mission: Analyzing Samples from the Edge of the Solar System
Don Brownlee 179

Paleobiology of Herbivorous Dinosaurs
Paul M. Barrett 207

Spin Transitions in Mantle Minerals
James Badro 231

Mercury Isotopes in Earth and Environmental Sciences
Joel D. Blum, Laura S. Sherman, and Marcus W. Johnson 249

Annu. Rev. Earth Planet. Sci. 2014.42:317-339. Downloaded from www.annualreviews.org
Access provided by Pennsylvania State University on 10/26/15. For personal use only.

Investigating Microbe-Mineral Interactions: Recent Advances in X-Ray and Electron Microscopy and Redox-Sensitive Methods
Jennyfer Miot, Karim Benzerara, and Andreas Kappler 271

Mineralogy of the Martian Surface
Bethany L. Ehlmann and Christopher S. Edwards 291

The Uses of Dynamic Earthquake Triggering
Emily E. Brodsky and Nicholas J. van der Elst 317

Short-Lived Climate Pollution
R.T. Pierrehumbert 341

Himalayan Metamorphism and Its Tectonic Implications
Matthew J. Kohn 381

Phenotypic Evolution in Fossil Species: Pattern and Process
Gene Hunt and Daniel L. Rabosky 421

Earth Abides Arsenic Biotransformations
Yong-Guan Zhu, Masafumi Yoshinaga, Fang-Jie Zhao, and Barry P. Rosen 443

Hydrogeomorphic Effects of Explosive Volcanic Eruptions on Drainage Basins
Thomas C. Pierson and Jon J. Major 469

Seafloor Geodesy
Roland Bürgmann and David Chadwell 509

Particle Geophysics
Hiroyuki K.M. Tanaka 535

Impact Origin of the Moon?
Erik Asphaug 551

Evolution of Neogene Mammals in Eurasia: Environmental Forcing and Biotic Interactions
Mikael Fortelius, Jussi T. Eronen, Ferhat Kaya, Hui Tang, Pasquale Raia, and Kai Puolamäki 579

Planetary Reorientation
Isamu Matsuyama, Francis Nimmo, and Jerry X. Mitrovica 605

Thermal Maturation of Gas Shale Systems
Sylvain Bernard and Brian Horsfield 635

Global Positioning System (GPS) and GPS-Acoustic Observations: Insight into Slip Along the Subduction Zones Around Japan
Takuya Nishimura, Mariko Sato, and Takeshi Sagiya 653

On Dinosaur Growth
Gregory M. Erickson 675

Annu. Rev. Earth Planet. Sci. 2014.42:317-339. Downloaded from www.annualreviews.org
Access provided by Pennsylvania State University on 10/26/15. For personal use only.

Diamond Formation: A Stable Isotope Perspective
Pierre Cartigny, Médéric Palot, Emilie Thomassot, and Jeff W. Harris 699

Organosulfur Compounds: Molecular and Isotopic Evolution from Biota to Oil and Gas
Alon Amrani 733

Indexes

Cumulative Index of Contributing Authors, Volumes 33–42 769

Cumulative Index of Article Titles, Volumes 33–42 774

Errata

An online log of corrections to *Annual Review of Earth and Planetary Sciences* articles may be found at http://www.annualreviews.org/errata/earth

Annu. Rev. Earth Planet. Sci. 2014.42:317-339. Downloaded from www.annualreviews.org
Access provided by Pennsylvania State University on 10/26/15. For personal use only.